JOURNAL OF GEOPHYSICAL RESEARCH, VOL. 100, NO. B4, PAGES 6329–6338, APRIL 10, 1995

Horizontal surface deformation due to dike emplacement in an elastic-gravitational layer overlying a viscoelastic-gravitational half-space

M. A. Hofton

Department of Geological Sciences, University of Durham, Durham, England

J. B. Rundle

Cooperative Institute for Research in Environmental Sciences, University of Colorado, Boulder

G. R. Foulger

Department of Geological Sciences, University of Durham, Durham, England

Abstract. We extend a technique previously used to model surface displacements resulting from thrust faulting in an elastic-gravitational layer over a viscoelastic-gravitational half-space to the case of dike emplacement. The method involves the calculation of the Green's functions for a dike point source contained in an elastic-gravitational layer over an elastic-gravitational half-space. The correspondence principle is then applied to introduce time dependence. The resultant Green's functions are integrated over the source region to obtain the near-field displacements. Several example calculations are presented involving 90°, 60°, and 30° dipping dikes, extending completely and partially through the elastic layer. We also illustrate the time dependent deformation due to buried dikes. Dikes extending completely through the elastic layer produce a larger-amplitude long-wavelength component than those extending partially through the elastic layer. Inflexion points are seen in the dike-normal horizontal deformation profiles when the base of the dike intersects the top of the half-space, providing a means of differentiating between vertical surface dikes extending completely and partially through the elastic layer. All results show that the use of a viscoelastic half-space underlying an elastic layer introduces a long-wavelength component into the deformation field that cannot be predicted by elastic half-space models.

Introduction

An important goal of modern crustal deformation studies is to understand the transient postevent ground deformation sometimes seen following large earthquakes and dike emplacement events. Stress relaxation in a nonelastic region situated below the surface elastic zone is one possible mechanism for transient strain [e.g., *Thatcher and Rundle*, 1979; *Thatcher et al.*, 1980; *Cohen*, 1984]. A second possible explanation is continued slip at depth on the fault or dike plane.

Elastic models involving dislocation sources in a homogeneous half-space [e.g., *Chinnery*, 1961; *Okada*, 1985] or in a layered half-space [e.g., *Jovanovich et al.*, 1974] cannot explain time dependent transient behavior. One method of introducing time dependence is by including a viscoelastic half-space. *Nur and Mavko* [1974], *Rundle and Jackson* [1977], *Spence and Turcotte* [1979], *Rundle* [1978, 1980], *Savage and Prescott* [1978], *Matsu'ura and Tanimoto* [1980], and others have studied the time dependent behavior with thrust or strike-slip sources. Authors dealing with dilatational sources include *Roth* [1993], who found a solution for an opening crack contained in a layered elastic half-space that could be extended to simulate a system of dikes, and *Heki et al.* [1993], who proposed a viscous diffusion model for post-diking stress relaxation at divergent plate boundaries.

We extend the work of *Rundle* [1980, 1981] to include the case of dike opening in an elastic layer overlying a viscoelastic half-space, the application of which will be especially useful in predicting transient deformation in areas of active tectonic rifting and at mid-ocean ridges. We limit the choice of materials in the viscoelastic region to those whose rheological properties have linear constitutive laws since even though the deformations are large, the strains are small as these depend on the small differences between time dependent displacements and the steady plate velocity. Because the strains are small, we can use a linear model; the nonlinear terms

Paper number 94JB03266.
0148-0227/95/94JB-03266$05.00

will all be negligible compared to the magnitude of the linear terms. A Maxwell rheology is also assumed which implies the inelastic region behaves as an elastic solid over short time periods and as a Newtonian fluid over long timescales. This is considered by the authors to be the most appropriate linear rheology for long-term deformation processes within the Earth.

We include gravitational effects in our calculations. For deformation at the surface of an elastic half-space, gravitational effects become significant over wavelengths greater than 1000 km [*Rundle*, 1980] but have little relevance to deformation near the source region. In viscoelastic structures, stresses in some regions of the Earth decrease as flow occurs: the initial elastic stresses induce flow in the medium, generating a change in the displacements and gravitational stresses as a result. Equilibrium is eventually attained between the gravitational and elastic stresses in the flowing region. However over short time intervals gravitational effects are small [*Rundle*, 1981], and the inclusion of gravitational effects is significant only when the event is assumed to reoccur, producing a cyclic distribution of events.

In this paper, surface displacements following dike emplacement are modeled using Green's functions. The solutions for the elastic-gravitational problem are first computed. Then the correspondence principle which relates the elastic-gravitational solution to the Laplace-transformed viscoelastic-gravitational solution is applied. Finally, the resultant Green's functions are integrated over the finite source region to obtain the time dependent, near-field displacements. A brief review of the method developed by *Rundle* [1980, 1981] is given here.

Solution to the Infinite Space Problem

Rundle [1981] found that for displacements resulting from a dip-slip event in a layered elastic-gravitational medium, self-gravitation effects arising from the nonzero value of G_0, the gravitational constant, were generally much smaller than gravitational effects relating to the surface acceleration, g. Making use of this, *Rundle* [1981] considered the governing equations [*Love*, 1911]

$$\nabla^2\vec{u}+\frac{1}{1-2\sigma}\nabla\nabla\cdot\vec{u}+\frac{\rho_0 g}{\mu}\nabla(\vec{u}\cdot\hat{e_z}) -\frac{\rho_0}{\mu}\nabla\phi-\frac{\rho_0 g}{\mu}\hat{e_z}\nabla\cdot\vec{u}=0, \quad (1)$$

$$\nabla^2\phi=-4\pi\rho_0 G_0\nabla\cdot\vec{u}, \quad (2)$$

where $\vec{u}$ is the perturbed displacement vector in the deformed cylindrical coordinate system (r,θ,z), ϕ is the gravitational potential in this coordinate system, $\hat{e_r},\hat{e_\theta}$, and $\hat{e_z}$ are the unit vectors, σ is Poisson's ratio, ρ_0 is the density and μ is the rigidity. As $z\rightarrow\infty$, all perturbed quantities are presumed to tend to zero, so setting $G_0=0$ implies ϕ is constant. In this case we may write

$$\nabla^2\vec{u}+\frac{1}{1-2\sigma}\nabla\nabla\cdot\vec{u}+\frac{\rho_0 g}{\mu}\nabla(\vec{u}\cdot\hat{e_z})-\frac{\rho_0 g}{\mu}\hat{e_z}\nabla\cdot\vec{u}=0. \quad (3)$$

Using the vector base

$$\vec{P_m} = J_m(kr)e^{im\theta}\hat{e_z}, \quad (4)$$

$$\vec{B_m} = \left(\frac{\partial J_m(kr)}{\partial kr}\hat{e_r}+im\frac{J_m(kr)}{kr}\hat{e_\theta}\right)e^{im\theta}, \quad (5)$$

$$\vec{C_m} = \left(im\frac{J_m(kr)}{kr}\hat{e_r}-\frac{\partial J_m(kr)}{\partial kr}\hat{e_\theta}\right)e^{im\theta}, \quad (6)$$

where $J_m(kr)$ are cylindrical Bessel functions, $i=\sqrt{-1}$, and k corresponds to the wave number in dynamical problems [cf. *Ben Menahem and Singh*, 1968], we can expand $\vec{u}$ in terms of equations (4) to (6) as

$$\vec{u}=\sum_{m=0}^{\infty}\int_0^{\infty}k\,dk[W_m(z)\vec{P_m}+U_m(z)\vec{B_m}+V_m(z)\vec{C_m}]. \quad (7)$$

The solution given by $V_m(z)$ is not considered as it is found to be identical to the solution in the nongravitating case. $U_m(z)$ and $W_m(z)$ are given by *Rundle* [1981] as

$$\begin{pmatrix}U_m(z)\\V_m(z)\end{pmatrix}=\begin{pmatrix}1\\p_1^+(k)\end{pmatrix}e^{a_1 z}+\begin{pmatrix}1\\p_1^-(k)\end{pmatrix}e^{-a_1 z} +k\begin{pmatrix}1\\p_2^+(k)\end{pmatrix}e^{a_2 z}+k\begin{pmatrix}1\\p_2^-(k)\end{pmatrix}e^{-a_2 z}, \quad (8)$$

where

$$\pm a_1 = \pm(k^2+k\eta\sqrt{\zeta})^{1/2}, \quad (9)$$

$$\pm a_2 = \pm(k^2-k\eta\sqrt{\zeta})^{1/2}, \quad (10)$$

$$\zeta = \frac{1-2\sigma}{2(1-\sigma)}, \quad (11)$$

$$p_j^{\pm}(k)=\pm 1-\frac{k\eta\sqrt{\zeta}}{(a_j+k)}\,\frac{1+\sqrt{\zeta}}{a_j-k\sqrt{\zeta}},\quad j=1,2, \quad (12)$$

and

$$\eta = \frac{\rho_0 g}{\mu}=\rho g, \quad (13)$$

$$\rho = \frac{\rho_0}{\mu}. \quad (14)$$

The gravitational wave number k_g, found by setting $a_2(k)=0$, is defined as

$$k_g=\eta\sqrt{\zeta}. \quad (15)$$

For $k<k_g$, a_2 is purely imaginary, and for $k>k_g$, a_2 is real.

Solution to the Layered Half-Space Problem

Rundle [1980] used a polar coordinate system (r,θ,z) with unit vectors $\hat{e_r},\hat{e_\theta}$, and $\hat{e_z}$, and with the z axis oriented down into the medium at the surface of a layered, elastic-gravitational half-space. The elastic moduli in the nth layer are denoted by λ_n and μ_n, and the

density by ρ_n. The solution in the nth layer is given by

$$\vec{u}^n = \sum_{m=0} \int_0^\infty k\,dk\ \vec{u}_m^n\ , \tag{16}$$

where $\vec{u}_m^n$ is given by

$$\vec{u}_m^n = x_m^n \vec{P}_m + y_m^n \vec{B}_m + z_m^n \vec{C}_m, \tag{17}$$

and the kernel functions x_m^n, y_m^n and z_m^n are

$$\begin{aligned} x_m^n &= -e^{-kz}A_{mn}^- + e^{kz}A_{mn}^+ + p_1^- e^{-a_1 z}B_{mn}^- \\ &\quad + p_1^+ e^{a_1 z}B_{mn}^+ + kp_2^- e^{-a_2 z}D_{mn}^- \\ &\quad + kp_2^+ e^{a_2 z}D_{mn}^+, \end{aligned} \tag{18}$$

$$\begin{aligned} y_m^n &= e^{-kz}A_{mn}^- + e^{kz}A_{mn}^+ + e^{-a_1 z}B_{mn}^- \\ &\quad + e^{a_1 z}B_{mn}^+ + ke^{-a_2 z}D_{mn}^- + ke^{a_2 z}D_{mn}^+, \end{aligned} \tag{19}$$

$$z_m^n = e^{-kz}C_{mn}^- + e^{kz}C_{mn}^+. \tag{20}$$

Here $\pm a_1$ and $\pm a_2$ are defined by equations (9) and (10). The same formulation is applied to the stresses across the layer boundaries to obtain similar expressions for the normal tractions across a plane.

As can be seen from equations (18) to (20), the problem can be divided into two separate parts, the "R" problem (that includes the x_m^n and y_m^n terms) and the "L" problem (that includes the z_m^n terms). The solutions to these problems are given by *Rundle* [1980, (equations 88–96)].

Source Functions

The source functions $[D_m]$ for the six elementary displacement dislocation sources have been derived by *Ben Menahem and Singh* [1968]. In the notation of *Singh* [1970], (jk) refers both to the direction of the force system and the normal to the plane across which it is applied. For a dike inclined at an angle ψ to the horizontal

$$(jk) = (3,3)\cos^2\psi + (2,2)\sin^2\psi - (2,3)\sin 2\psi, \tag{21}$$

with each component given by

$$\begin{aligned} (jk) = (2,2): &\quad (D_0)_1 = 2\gamma(3\delta - 1)/(\delta + 1), \\ &\quad (D_0)_4 = \mu\gamma(7\delta - 1)/(\delta + 1), \\ &\quad (D_2)_4 = \mu\gamma, \\ &\quad (D_2^L)_2 = -2\mu\gamma i, \\ (jk) = (3,3): &\quad (D_0)_1 = 2\gamma, \\ (jk) = (2,3): &\quad (D_1)_2 = -2\gamma i, \\ &\quad (D_1^L)_1 = -2\gamma. \end{aligned} \tag{22}$$

Here $\gamma = \Delta U\, d\Sigma/4\pi$, where ΔU is the relative displacement across the crack, $d\Sigma$ is an element of area on the crack, and δ=1/(3-4σ).

Hence we have three different source function contributions to the diking problem, one describing opening in the vertical direction ($m = 0$), a second describing opening in the horizontal direction ($m = 2$) and a shearing component ($m = 1$). Using equations (16) and (17) and summing these three contributions, the displacement at the surface may be written as

$$\begin{aligned} \vec{u} = \int_0^\infty k\,dk \Big\{ &\left[x_0^{1(33)}(0)\vec{P}_0 + y_0^{1(33)}(0)\vec{B}_0\right]\cos^2\psi \\ &+ \left[x_0^1(0)\vec{P}_0 + y_0^1(0)\vec{B}_0 + x_2^1(0)\vec{P}_2 + y_2^1(0)\vec{B}_2 \right. \\ &\left. + z_2^1(0)\vec{C}_2\right]\sin^2\psi - \left[x_1^1(0)\vec{P}_1 + y_1^1(0)\vec{B}_1 \right. \\ &\left. + z_1^1(0)\vec{C}_1\right]\sin 2\psi \Big\}. \end{aligned} \tag{23}$$

The superscript (33) distinguishes the kernel functions of the $(jk) = (3,3)$ component from the $(jk) = (2,2)$ component. Substituting equations (4) to (6) for $\vec{P}_m$, $\vec{B}_m$ and $\vec{C}_m$, replacing $e^{im\theta}$ and $ie^{im\theta}$ by $\cos m\theta$ and $-\sin m\theta$, respectively, to obtain the real part, and splitting the displacement vector into its three components, we obtain

$$\begin{aligned} u_r = -\int_0^\infty k\,dk \Big\{ &y_0^{1(33)}(0)J_1(kr)\cos^2\psi \\ &+ \left(y_0^1(0)J_1(kr) - \left[y_2^1(0)\left(\frac{J_1(kr) - J_3(kr)}{2}\right)\right.\right. \\ &\left.\left. - \frac{1}{i}z_2^1(0)\left(\frac{J_1(kr) + J_3(kr)}{2}\right)\right]\cos 2\theta\right)\sin^2\psi \\ &- \left[\frac{1}{i}y_1^1(0)\left(\frac{J_0(kr) + J_2(kr)}{2}\right)\right. \\ &\left. + z_1^1(0)\left(\frac{J_0(kr) + J_2(kr)}{2}\right)\right]\sin\theta\sin 2\psi \Big\}, \end{aligned} \tag{24}$$

$$\begin{aligned} u_\theta = \int_0^\infty k\,dk \Big\{ &\left[\frac{1}{i}z_2^1(0)\left(\frac{J_1(kr) - J_3(kr)}{2}\right)\right. \\ &\left. - y_2^1(0)\left(\frac{J_1(kr) + J_3(kr)}{2}\right)\right]\sin 2\theta\sin^2\psi \\ &+ \left[\frac{1}{i}y_1^1(0)\left(\frac{J_0(kr) + J_2(kr)}{2}\right)\right. \\ &\left. + z_1^1(0)\left(\frac{J_0(kr) - J_2(kr)}{2}\right)\right]\cos\theta\sin 2\psi \Big\}, \end{aligned} \tag{25}$$

$$\begin{aligned} u_z = \int_0^\infty k\,dk \Big\{ &x_0^{1(33)}(0)J_0(kr)\cos^2\psi \\ &+ x_0^1(0)J_0(kr)\sin^2\psi + x_2^1(0)J_2(kr)\cos 2\theta\sin^2\psi \\ &+ \frac{1}{i}x_1^1(0)J_1(kr)\sin\theta\sin 2\psi \Big\}. \end{aligned} \tag{26}$$

Equations (24) to (26) give the solution to the elastic-gravitational problem of a point nucleus of dilation in an elastic-gravitational layer over an elastic-gravitational half-space.

Introduction of Viscoelasticity

As the first step, the correspondence principle of linear viscoelasticity is applied [*Lee*, 1955]. This requires that the elastic quantities λ and μ in each component of the elastic solution be replaced by their Laplace trans-

formed quantities $s\bar{\lambda}(s)$ and $s\mu(s)$ to obtain $\bar{u}(s)$ where the bar signifies the Laplace-transformed quantity and s is the parameter conjugate to time. Then $\bar{u}(s)$ is inverted to give $u_v(t)$, the solution to the viscoelastic problem. The technique used to perform the inversion involves the Prony series where the function $u_v(t)$ is approximated by a function $u_v^\star(t)$ composed of a series of decaying exponentials. Following *Schapery* [1961] and *Cost* [1964] we set

$$u_v(t) \cong \sum_{ij}^{N} A_i \tau_i (1 - e^{-t/\tau_i}) = u_v^\star(t), \qquad (27)$$

where $\cong$ means "approximately equal to in the least squares sense" and where $\{\tau_{ij}\}$ is a set of N relaxation times. In this problem we set

$$\{\tau_{ij}\} = \{0.5\tau_a, \tau_a, 5\tau_a, 10\tau_a, 50\tau_a, 100\tau_a\},$$

where τ_a, the characteristic relaxation time, is defined by $\tau_a = 2\eta/\mu_h$ in which η is the viscosity of the Maxwell fluid and μ_h is the elastic modulus of the half-space. The A_i are then a set of unknown constants to be determined. This approximation method has the advantage of smooth time domain results in the time interval required and involves as few function evaluations as possible. The error obtained using the numerical method is thus minimized. Then $u_v^\star(t)$ can be integrated over the source region to obtain the required solution.

Results

Post-diking horizontal deformation is predicted over timescales of 0 to $50\tau_a$. Effects due to the inclusion of gravity and from the variation of the fault parameters μ_h, D, W, and ψ (Figure 1) are studied. Note that the figures (Figures 2 to 4, 6, 8 to 10) illustrating postdiking displacements where gravitational effects are not included show nondimensional horizontal motion perpendicular to the dike plane, i.e., in the y direction, over an area scaled in terms of H. The figures (Figures 5 and 7) which include gravitational effects do not have their horizontal motion and lengths scaled in a similar manner. In the gravitational problem several independent length scales now exist: H, the layer thickness, and k_g^L and k_g^H, the gravitational wave numbers for the layer and half-space. A nondimensionalizing of the kernel functions for the gravitational case results in a ratio of gravitational effects to elasticity effects, e.g., $\rho g H/\mu$ [*Rundle*, 1982].

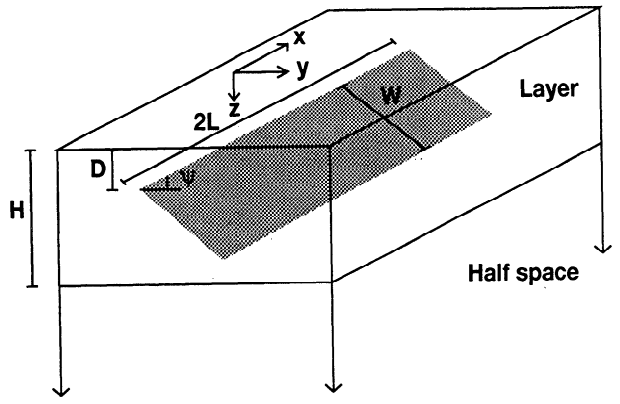

Figure 1. Geometry and coordinate system for a rectangular, dipping dike in an elastic-gravitational layer over a viscoelastic-gravitational half-space. H is the thickness of the layer, D is the depth of the dike, $2L$ is the along strike length, W is the downdip width, and ψ is the dip.

The case of a vertical dike extending completely through the elastic layer ($W/H = 1$) is shown in Figure 2. The predicted codiking deformation is large close to the source and decreases as the distance from the source increases. The postdiking response behaves in the opposite sense with little deformation predicted in the near-source region and substantial deformation at distances several dike widths from the source. Rebound of the nonelastic region in response to the rapid outward movement from the diking leads to the formation of an inflexion in the displacement field close to the source. The amplitude of the postdiking deformation field is increased as a result of increasing μ_h (compare Figures 2 and 3). This also leads to the formation of a more pronounced peak in the field several dike widths away from the source. In addition, increasing μ_h increases the magnitude of the completion time of the postdiking deformation. Viscosity is directly proportional to rigidity; hence increasing μ_h implies that the viscoelastic region has become less "fluid" and responds more slowly to postdiking stress changes but with a larger magnitude response. Decreasing the downdip width of the dike such that it extends halfway through the elastic layer from the surface produces minimal differences in the codiking deformation field. (compare Figures 3 and 4). However, the postdiking deformation field now has a more pronounced peak related to the thickness of the elastic layer, and it has no inflexion in the near-source region. The presence of this inflexion in the displacement field is a direct consequence of the base of the dike touching the top of the half-space. Decreasing the downdip width of the surface dike by a small fraction removes the presence of the inflexion from the postdiking deformation fields. Hence the case of a dike extending completely through the elastic layer can be distinguished from the case of a surface dike which extends partially through the elastic layer by inspection of the postdiking deformation fields. The inclusion of gravitational effects produces no significant differences in the horizontal deformation field over all time intervals for the dike of downdip width H, but decreasing the downdip width of the dike results in a significant attenuation of the long time interval postdiking deformation fields (compare Figures 4 and 5).

Burying the dike has a profound effect on the predicted postdiking deformation field. The codiking response has a smaller amplitude than that predicted using the surface dike sources, with the maximum displacement occurring at a greater distance from the source. The inflexion seen in the near-source region

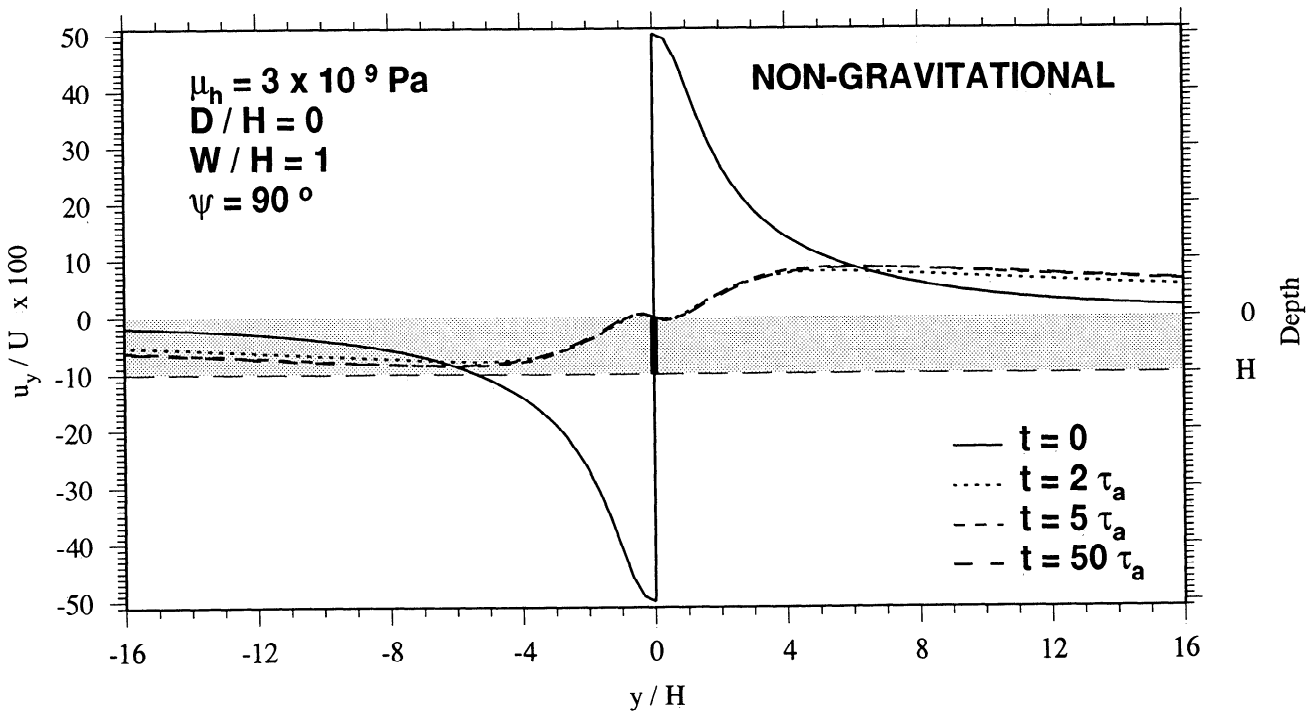

Figure 2. Nondimensional surface horizontal deformation against distance normal to a dike extending completely through the elastic layer. Model parameters are $H = 30$ km, $2L = 20H/3$, $\rho_l = \rho_h = 3.0$ g/cm^3, $\mu_l = \lambda_l = \lambda_h = 3\text{x}10^{10}$ Pa, $\mu_h = 3\text{x}10^9$ Pa, $D/H = 0$, $W/H = 1$, and $\psi = 90°$. The codiking response is calculated using the formulae of *Okada* [1985] for a dike in an elastic half-space where $\mu = \lambda = 3\text{x}10^{10}$ Pa. The shaded area represents the elastic-gravitational layer, the horizontal dashed line is the layer half-space boundary, and the heavy solid line shows the dike geometry. The solid curve is the initial elastic (codiking) response, and the dashed curves represent the deformation due to viscoelastic stress relaxation after $2\tau_a$, $5\tau_a$, and $50\tau_a$. Each displacement profile has been evaluated at the midpoint of the fault plane.

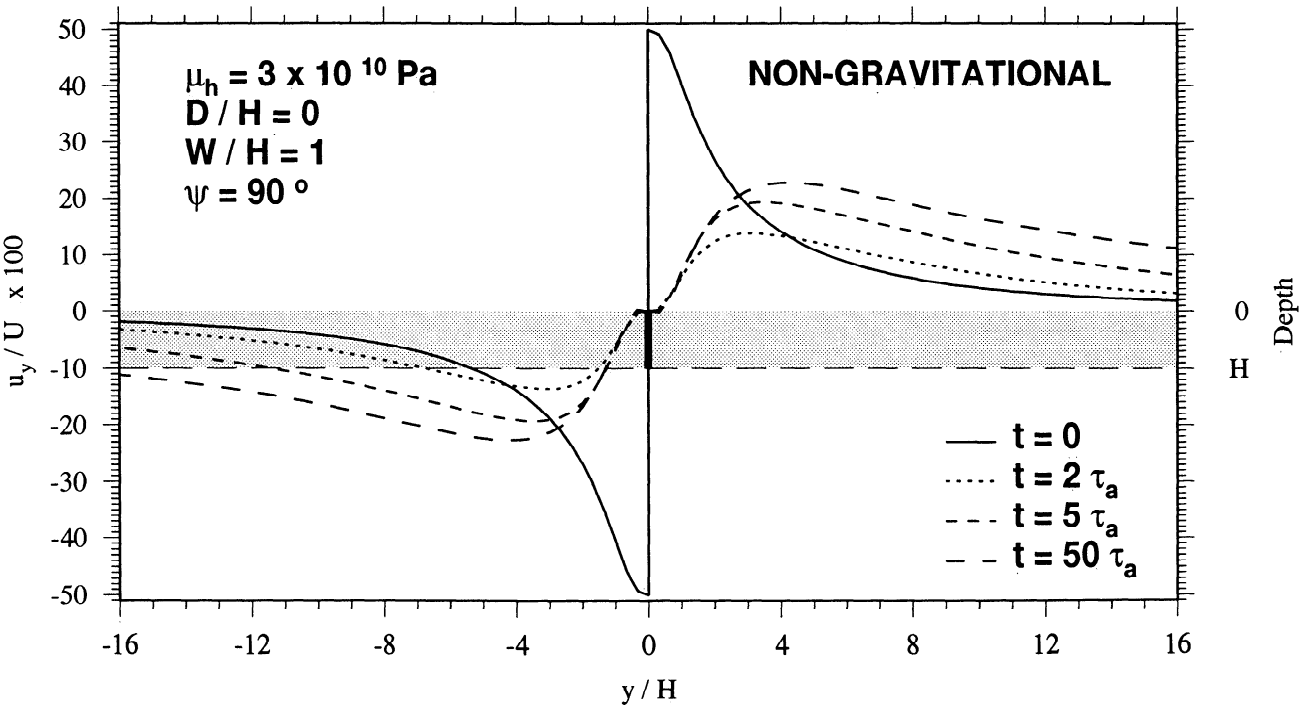

Figure 3. Same as Figure 2 except $\mu_h = 3\text{x}10^{10}$ Pa.

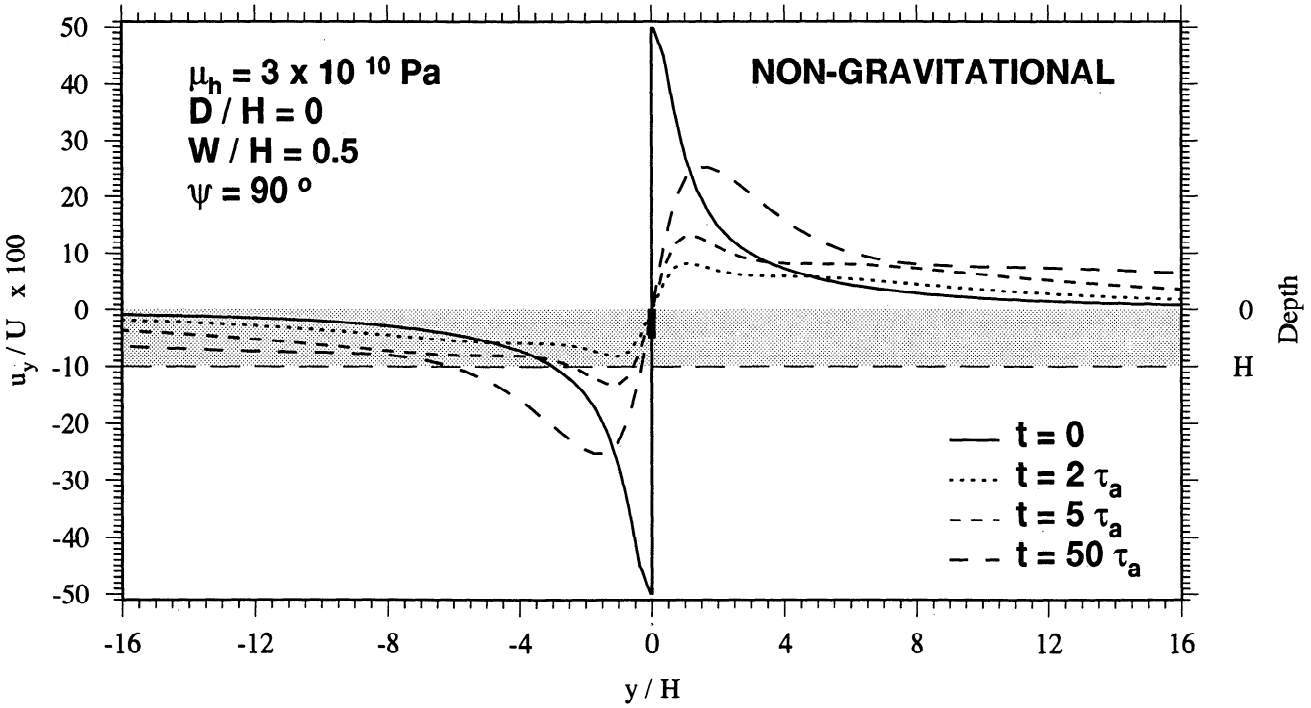

Figure 4. Same as Figure 2 except $D/H = 0$, $W/H = 0.5$, and $\mu_h = 3\text{x}10^{10}$ Pa.

of the postdiking deformation field (Figure 6) is of a larger amplitude and covers a greater area than that predicted for a surface dike of twice the downdip width. The inclusion of gravitational effects results in an attenuation of the deformation field (compare Figures 6 and 7); however, when compared to the surface diking case these effects become apparent over a much shorter timescale. This difference in time scales is due to the closeness of the dike end to the halfspace. The stresses die off from the fault ends like $1/r$, so for the case of a buried dike extending to the base of the elastic layer the halfspace will experience shorter wavelength stresses and faster stress relaxation than if the dike extended from the surface to the midpoint of the elastic layer [*Rundle*, 1982].

The dominant effect of altering the dip of the dike

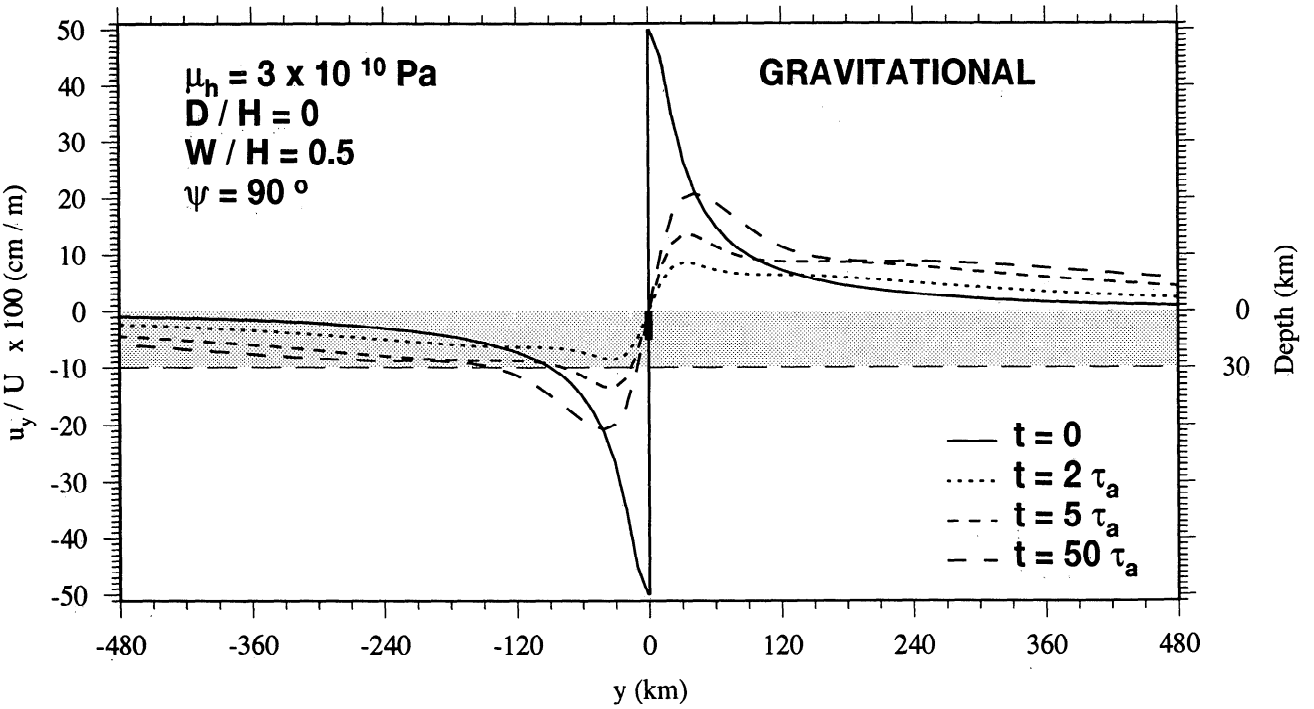

Figure 5. Same as Figure 4 except gravitational effects are included in the model. Surface deformation is now in centimeters per meter of opening.

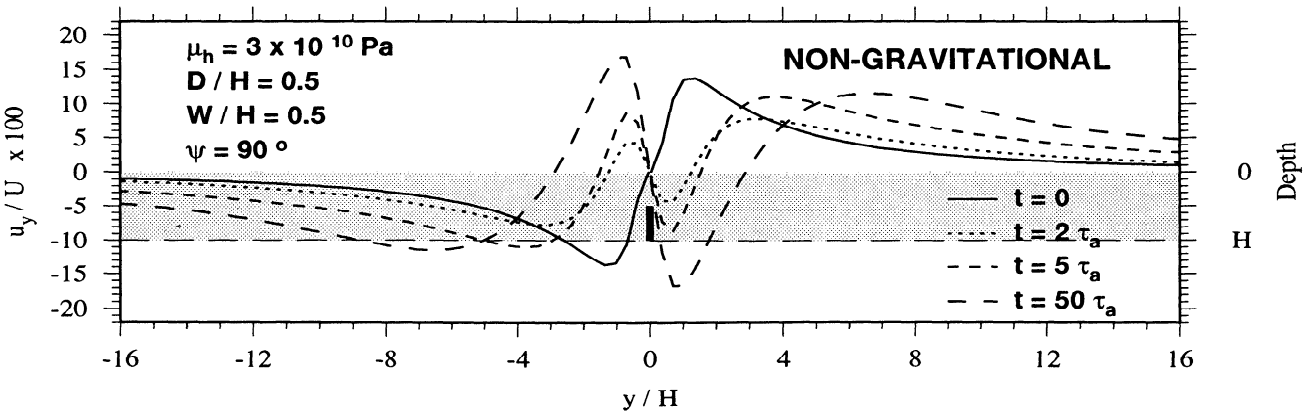

Figure 6. Same as Figure 2 except $D/H = 0.5$, $W/H = 0.5$, and $\mu_h = 3\text{x}10^{10}$ Pa.

is the formation of an asymmetrical deformation field in both the codiking and postdiking response (compare Figures 4 and 8 and Figures 6 and 9). Other features are similar to those observed in the corresponding vertical dike cases with the asymmetric features being introduced by the dip of the dike. Increasing the dip of the dike increases the scale of the asymmetrical effect (compare Figures 8 and 10). The inclusion of gravitational effects into these cases results in the same effects as those observed for the vertical dike case. That is, for the surface dike no apparent differences are observed until longer time periods, and for the buried dike these differences occur within shorter timescales.

Regions of uplift and subsidence can be associated with areal strain compression and expansion patterns [*Bilham and King*, 1989]. The horizontal strain field is given by the derivative of the horizontal deformation curves; hence regions of uplift and subsidence can be inferred. A dike extending completely through the elastic layer produces uplift above the dyke, no appreciable motion either side of the dike, i.e., in the flank zones, and uplift further away. No appreciable motion is predicted in the far field. This pattern is repeated for a buried dike extending to the base of the elastic layer, except the flank zones now undergo subsidence. A surface dike extending halfway through the layer produces uplift of the flank zones with subsidence elsewhere and no appreciable motion in the far field.

Summary and Discussion

A previous method is extended in order to calculate the horizontal postdiking surface displacements as a result of a dike emplacement in an elastic layer above a viscoelastic half-space. The effects of gravity can be included in both the layer and the half-space but are found to produce minimal differences in the displacement fields until longer time intervals are considered. In addition, results indicate that it is possible to determine whether a dike extends completely or partially through the elastic layer by an inspection of the postdiking deformation fields.

The boundary conditions contained in the present version of the model, however, do not account for data that are affected by repeated events. The method appropriate to these circumstances is outlined by *Savage and Prescott* [1978], and the application of this will form a particularly valuable tool for interpreting observed geodetic horizontal surface deformation in areas of active tectonic rifting and for forward modeling at mid-ocean ridges. One region in which the model is currently applicable is in northeast Iceland where a

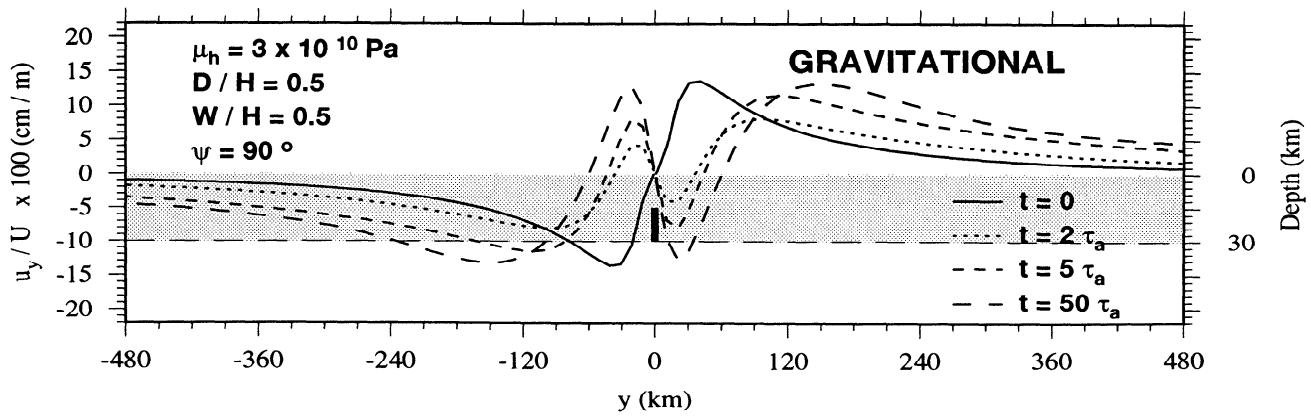

Figure 7. Same as Figure 6 except gravitational effects are included in the model. Surface deformation is now in centimeters per meter of opening.

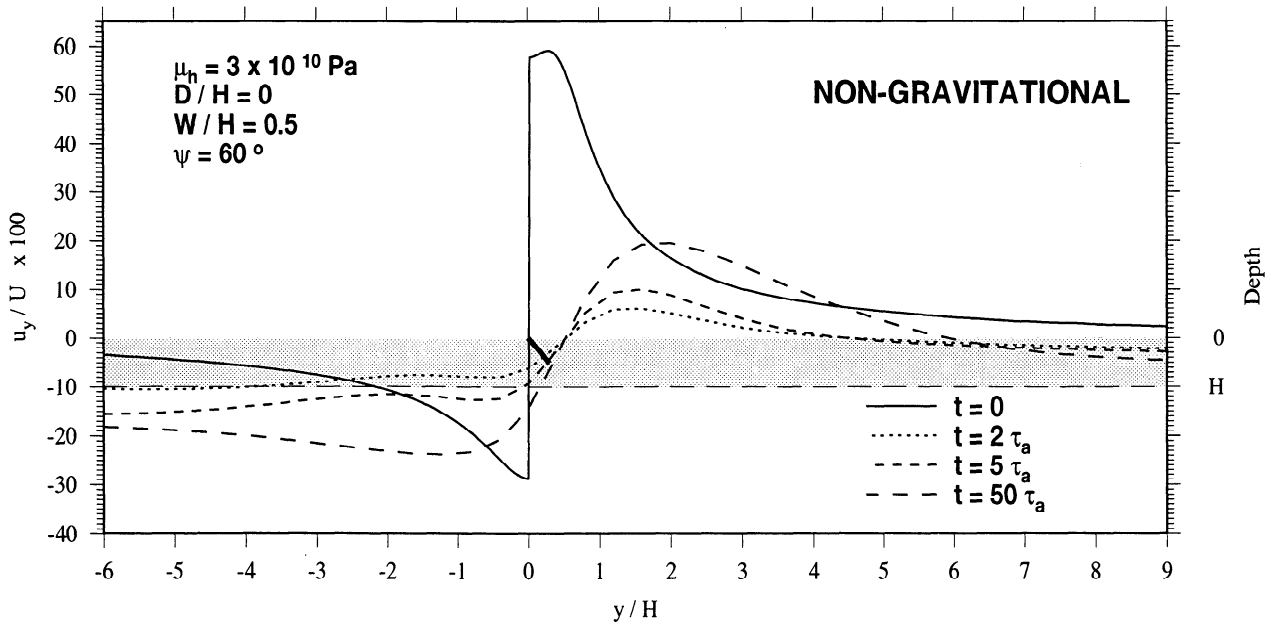

Figure 8. Same as Figure 2 except $\psi = 60°$, $D/H = 0$, $W/H = 0.5$, and $\mu_h = 3\text{x}10^{10}$ Pa.

major rifting episode commenced in 1975. In the following decade up to 8 m of crustal widening occurred along an 80 km-long-section of the accretionary plate boundary [*Björnsson*, 1985]. Repeated geodetic surveying results in this area using Global Positioning System (GPS) satellite surveying [*Heki et al.*, 1993; *Jahn et al.*, 1994] have revealed a horizontal deformation field that shows a clear postdiking transient signal that may be attributable to viscoelastic asthenospheric relaxation.

Furthermore, this model predicts the presence of a long-wavelength component in the postdiking deformation field following a single event, a result also obtainable by modeling continued diking at depth in an elastic half-space. One possible distinction between these two models lies in the analysis of the distribution of observed deformation with time. Here we demonstrate a nonlinear spatial variation of displacement with time. For a similar distribution of displacements to occur using the continued diking at depth in an elastic half-space hypothesis, a dike continually evolving in depth, downdip width, and length would have to be incorporated into the model. Data sets of a sufficiently high quality, for example, the northeast Iceland GPS data set [*Heki et al.*, 1993; *Jahn et al.*, 1994], are now becoming avail-

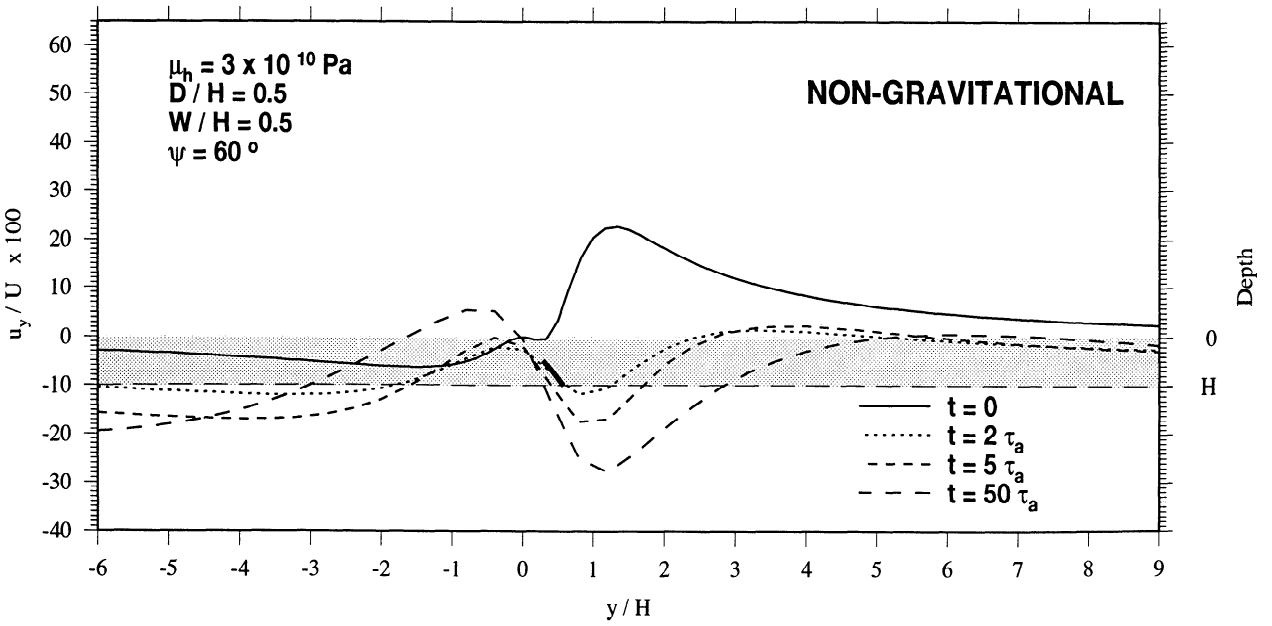

Figure 9. Same as Figure 2 except $\psi = 60°$, $D/H = 0.5$, $W/H = 0.5$, and $\mu_h = 3\text{x}10^{10}$ Pa.

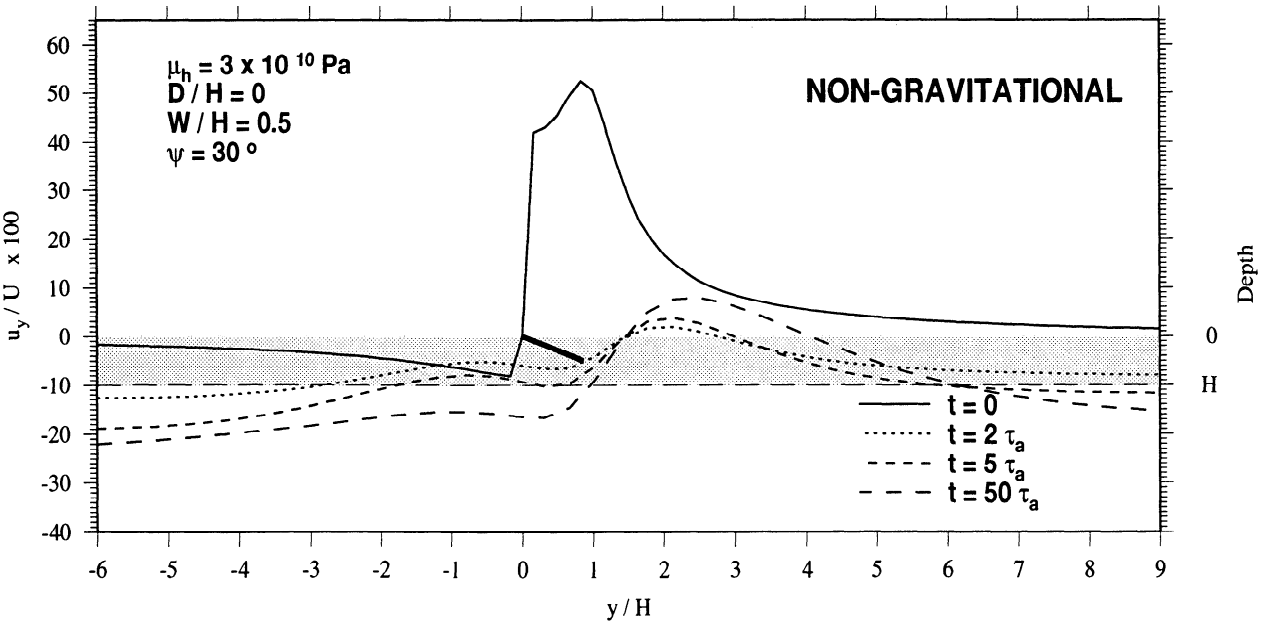

Figure 10. Same as Figure 2 except $\psi = 30°$, $D/H = 0$, $W/H = 0.5$, and $\mu_h = 3\text{x}10^{10}$ Pa.

able, enabling the possibility of distinguishing between these two methods. If a difference can be detected, then this will lead to a better understanding of the physical processes responsible for plate boundary processes.

Acknowledgments. The authors wish to thank J. C. Savage, R. S. Stein, S. C. Cohen and A. Donellan for their careful reviews.

References

Ben-Menahem, A., and S. J. Singh, Multipolar elastic fields in a layered half-space, *Bull. Seismol. Soc. Am., 58*, 1519–1572, 1968.

Bilham, R., and G. King, The morphology of strike-slip faults: Examples from the San Andreas fault, California, *J. Geophys. Res., 94*, 10,204–10,216, 1989.

Björnsson, A., Dynamics of rifting in NE Iceland, *J. Geophys. Res., 90*, 10,151–10,162, 1985.

Chinnery, M. A., Deformation of the ground around surface faults, *Bull. Seismol. Soc. Am., 51*, 355–372, 1961.

Cohen, S. C., Postseismic deformation due to subcrustal viscoelastic relaxation following dip-slip earthquakes, *J. Geophys. Res., 89*, 4538–4544, 1984.

Cost, T. L., Approximate Laplace transform inversions in viscoelastic stress analysis, *AIAA J., 2*, 2157–2166, 1964.

Jahn, C.-H., G. Seeber, G. R. Foulger, and P. Einarsson, GPS epoch measurements spanning the mid-Atlantic plate boundary in northern Iceland 1987–1990, in *Gravimetry and Space Techniques Applied to Geodynamics and Ocean Dynamics, Geophys. Monogr. Ser., vol. 82*, edited by B. E. Schutz et al., pp. 109–123, AGU, Washington, D. C., 1994.

Jovannovich, D. B., M. I. Husseini, and M. A. Chinnery, Elastic dislocations in a layered half space, I, Basic theory and numerical methods, *Geophys. J. R. Astron. Soc., 39*, 205–217, 1974.

Heki, K., G. R. Foulger, B. R. Julian and C.-H. Jahn, Plate dynamics near divergent boundaries: Geophysical implications of postrifting crustal deformation in NE Iceland, *J. Geophys. Res., 98*, 14279–14297, 1993.

Lee, E. H., Stress analysis in viscoelastic bodies, *J. Appl. Mech., 13*, 183–190, 1955.

Love, A. E. H., *Some Problems of Geodynamics*, Cambridge University Press, New York, 1911.

Matsu'ura, M., and T. Tanimoto, Quasi-static deformations due to an inclined, rectangular fault in a viscoelastic half-space, *J. Phys. Earth., 28*, 103–118, 1980.

Nur, A., and G. Mavko, Postseismic viscoelastic rebound, *Science, 183*, 204–206, 1974.

Okada, Y., Surface deformation due to shear and tensile faults in a half-space, *Bull. Seismol. Soc. Am., 75*, 1135–1154, 1985.

Roth, F., Deformations in a layered crust due to a system of cracks: Modeling the effect of dike injections or dilatancy, *J. Geophys. Res., 98*, 4543–4551, 1993.

Rundle, J. B., Viscoelastic crustal deformation by finite, quasi-static sources, *J. Geophys. Res., 83*, 5937–5945, 1978.

Rundle, J. B., Static elastic-gravitational deformation of a layered half-space by point couple sources, *J. Geophys. Res., 85*, 5354–5363, 1980.

Rundle, J. B., Vertical displacements from a rectangular fault in layered elastic-gravitational media, *J. Phys. Earth., 29*, 173–186, 1981.

Rundle, J. B., Viscoelastic-gravitational deformation by a rectangular thrust fault in a layered earth, *J. Geophys. Res., 87*, 7787–7796, 1982.

Rundle, J. B., and D. D. Jackson, A three dimensional viscoelastic model of a strike slip fault, *J. Geophys. Res., 49*, 575–592, 1977.

Savage, J. C., and W. H. Prescott, Asthenosphere readjustment and the earthquake cycle, *J. Geophys. Res., 83*, 3369–3376, 1978.

Schapery, R. A., Approximate methods of transform inversion for viscoelastic stress analysis, *Proc. U.S. Natl. Congr. Appl. Mech., 4th*, 1075–1085, 1961.

Singh, S. J., Static deformation of a multilayered half-space by internal sources, *J. Geophys. Res., 75*, 3257–3263, 1970.

Spence, D. A., and D. L. Turcotte, Viscoelastic relaxation of cyclic displacements on the San Andreas fault, *Proc. R. Soc. London A, 365*, 121–144, 1979.

Thatcher, W., and J. B. Rundle, A model for the earthquake

cycle in underthrust zones, *J. Geophys. Res., 84*, 5540–5556, 1979.

Thatcher, W., T. Matsuda, T. Kato, and J. B. Rundle, Lithospheric loading by the Riku-U earthquake, northern Japan: Implications for plate flexure and asthenospheric rheology, *J. Geophys. Res., 85*, 6429–6435, 1980.

G. R. Foulger and M. A. Hofton, Department of Geological Sciences, University of Durham, South Road, Durham, DH1 3LE, England. (email: m.a.hofton@durham.ac.uk)

J. B. Rundle, Cooperative Institute for Research in Environmental Sciences, University of Colorado, Boulder, CO 80309.

(Received April 26, 1994; revised November 28, 1994; accepted December 6, 1994.)